

## Short Note

# Constituent Energy of Regional Seismic Coda

by Tae-Kyung Hong and William Menke

**Abstract** Seismic coda is composed of scattered wavelets originated from various heterogeneities. The phase composition of regional seismic coda still remains unknown, despite its use for several decades. This is caused partly because the ray paths of scattered wavelets in coda are not on the great-circle path between a source and receiver. We examine the constituent original phases of regional coda with the help of a source-array analysis. A set of uniform sources that are essential for a source-array analysis is organized with underground nuclear explosions. Strong *Rg*-origin energy is observed in the coda at frequencies of 0.2–0.8 Hz, and it lasts more than 700 sec until the end of records. The coherent energy in the coda reduces with frequency. It constitutes about 20% of the total coda energy at frequencies of 0.2–0.4 Hz, and 12% at frequencies of 0.4–0.8 Hz. The other 80% of coda energy in 0.2–0.8 Hz is mixed with complex phases from various untraceable origins. The *Rg* energy is the most influential component in the construction of low-frequency regional coda. On the other hand, the coda at higher frequencies, 0.8–3.2 Hz, is observed to be mixed with complex phases that cause the wave field to be diffused. The observation of *Rg*-origin energy at the regional coda suggests that scattered energy from phase coupling of *Rg* is not significant compared to *Rg*-to-*Rg* scattered energy.

## Introduction

Seismic coda is composed of multipathing wavelets that are scattered from heterogeneities in the Earth. This seismic coda is observed at any distance, including local, regional, and teleseismic distances. High-frequency seismic coda is particularly well observed in local and regional distances. The strong excitation of local and regional coda suggests the presence of significant scatterers in the crust and upper mantle. The seismic coda, however, can hardly be used for a ray-based inversion due to the difficulty in identifying the ray path and phase of constituent wavelet. This feature leaves most seismic coda less used than direct phases.

Stochastic approaches have been applied often for coda analysis. The stochastic approaches determine the properties of heterogeneities in the medium from coda envelopes (Sato and Fehler, 1998; Hong *et al.*, 2005). Array data, in particular, were found to be useful for the stochastic analyses that allow stable measurement of coda properties (Sato and Fehler, 1998; Hong *et al.*, 2005). The crustal and mantle heterogeneities in the Earth could be characterized using the stochastic approaches (Capon, 1974; Hedlin *et al.*, 1997; Nishimura *et al.*, 2002).

Another important feature of coda is that the coda becomes diffusive with time because of the influence of multiple scattering (Aki and Chouet, 1975; Shapiro *et al.*, 2000; Hennino *et al.*, 2001). The properties of the source and media

could be estimated from diffusive coda (e.g., Mayeda and Walter, 1996; Hoshiya, 1997; Bianco *et al.* 1999). These coda characteristics were confirmed by various numerical and theoretical studies (Frankel and Wennerberg, 1987; Korn, 1993; Yoshimoto *et al.*, 1997; Sato and Fehler, 1998).

Despite these magnificent advances in coda analysis, however, many aspects of coda still remain unresolved. A prominent question is how the regional seismic coda is composed. Unlike local seismic records, regional seismic records display onsets of various regional phases (e.g., *Pn*, *Sn*, *Pg*, *Lg*, *Rg*). All of these regional phases can excite scattered wavelets when they interact with heterogeneities in the crust and mantle lid. However, the relative contribution of each regional phase on the construction of regional coda is rarely known. This unanswered problem, thus, leaves difficulty in the interpretation of observed regional coda. This, as a result, causes limited analysis of regional coda to inference of seismic properties of media. Thus, it is highly required to investigate the phase composition of regional coda.

The original phases of wavelets constituting regional coda can be investigated by examining wave fields from clustered events with help of a source-array analysis, which uses the reciprocity theorem (Aki and Richards, 1980; Spudich and Bostwick, 1987; Nowack and Chen, 1999; Hong and Xie, 2005). A set of uniform sources is essential for such

a source-array-based approach. However, uniform sources are hard to find in natural earthquakes, because source properties are often different—event by event—even on the same fault plane.

Underground nuclear explosions (UNEs) are good alternative sources. The UNEs not only have uniform source properties, but also are clustered in small areas. In addition, a full set of typical regional phases develop well from a UNE (Hong and Xie, 2005). These features enable us to study the phase composition of regional coda from a source-array analysis based on UNE records. In this article, we present the phase composition of regional coda in terms of original phases and examine its nature of frequency-dependent phase composition. Also, we discuss the potential of regional seismic coda for a study of crustal and upper-mantle structures with discussion of recent observations.

### Data and Geology

We used regional seismic records for UNEs at the Balapan test site during 1968–1989 (Fig. 1). The seismograms were recorded at the Borovoye seismic station, Kazakhstan, which is located at ~690 km in ~N304°E from the Balapan test site. The magnitudes,  $m_b$ , of the UNEs range between 4.8 and 6.2. High-precision UNE locations and origin times are available from various sources (National Nuclear Centre of the Republic of Kazakhstan [NNCRK], 1999; Kim *et al.*, 2001; Thurber *et al.*, 2001).

The recording system of BRV is composed of a set of vertical short-period seismometers that have various amplification rates (Kim *et al.*, 2001; Hong and Xie, 2005). We analyze seismograms from displacement seismometers with

a sensor type of SKM-3, which has a natural period of 2.0 sec and sampling rates of 0.032 and 0.096 sec (Fig. 2) (Kim *et al.*, 2001). We analyze high-gain records for a study of phase composition of regional coda to avoid digital round-off error. The number of records is 35 (Fig. 1). These high-gain record sections have been rarely analyzed in other studies because they display only coda sections clearly. We check every time section, and confirm that every time record is not contaminated by any noticeable interference of waves from other extraneous sources.

The  $P$ - and  $S$ -wave velocities in Kazakhstan increase gradually with depth, and reach 8.0 and 4.7 km/sec at the mantle lid (Quin and Thurber, 1992). The crustal basement on the great-circle path from the source region to the observatory is composed of Precambrian and early Palaeozoic hard rocks (Levashova *et al.*, 2003). This high  $Q$  crustal structure excites seismic records with high signal-to-noise ratios. The upper crust in the northeastern part of the Balapan test site has a lower shear velocity by ~0.4 km/sec than that in the southwestern part because of difference in surface geology (Ringdal *et al.*, 1992; Bonner *et al.*, 2001). Hong and Xie (2005) have recently reported that the  $S_n$  wave from the lower-velocity region (northeastern region) is stronger than that from the higher-velocity region (southwestern region). In this study, we analyze only the records from the southeastern region to avoid the influence of surface geology at the source region.

### Method

We apply a frequency–wavenumber ( $f$ - $k$ ) method to the BRV records for the Balapan UNEs. The  $f$ - $k$  method has been

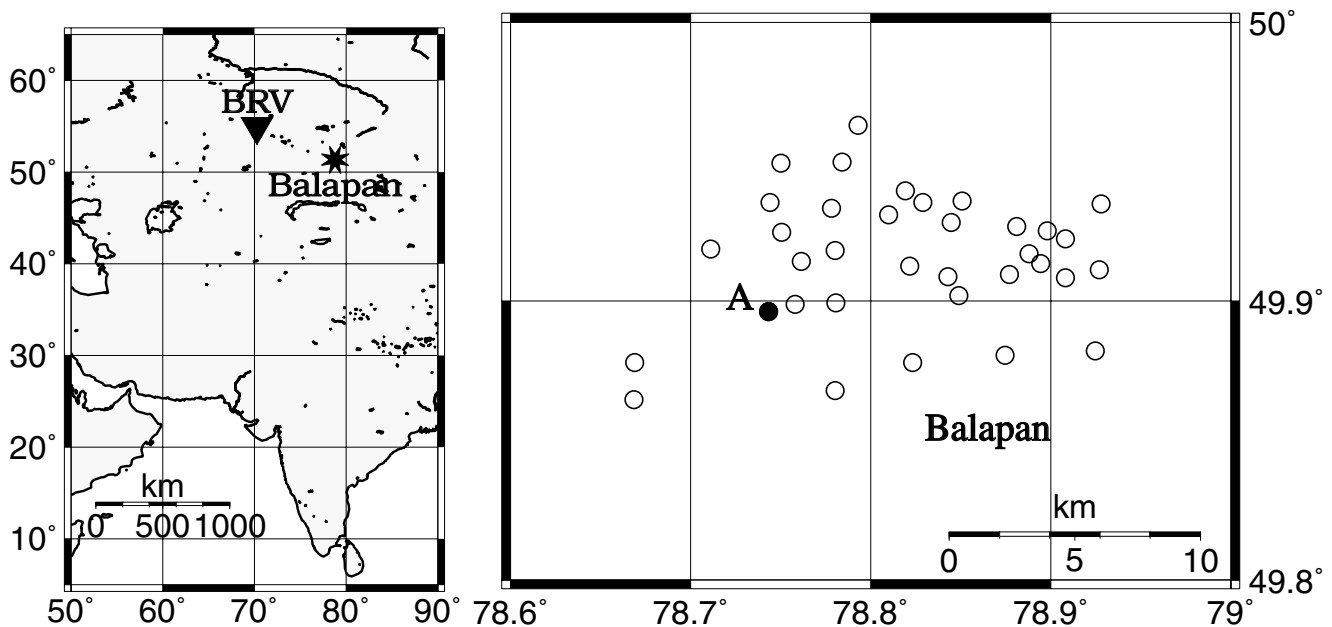


**Figure 1.** Map of the Borovoye seismic station (BRV) and nuclear explosions at the Balapan test site. The nuclear explosions that are used as source arrays in this study are marked with circles (35 events). The source-array aperture is about 19 km in the longitudinal direction.

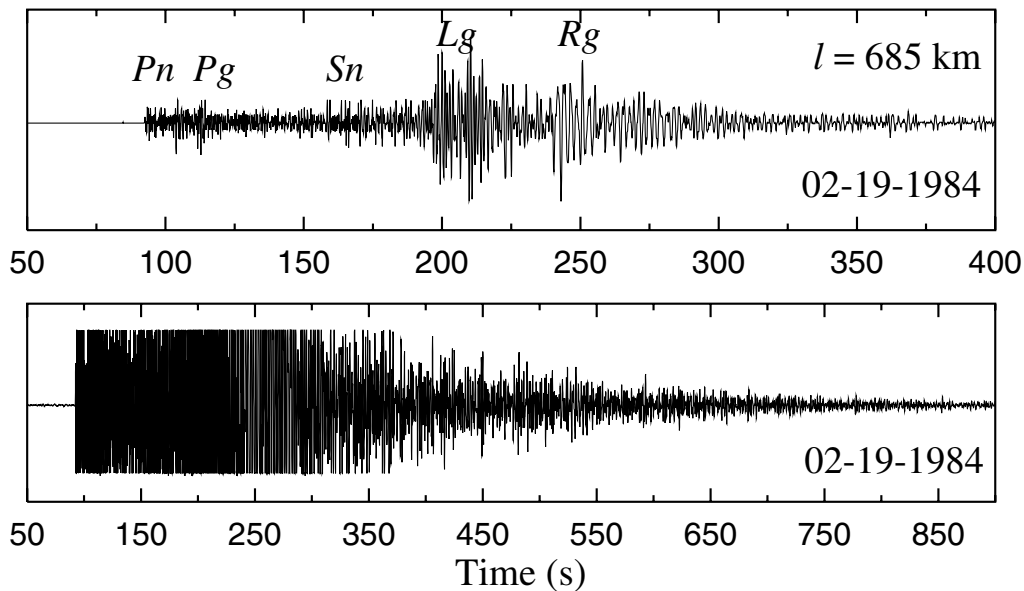


**Figure 2.** Vertical seismic waveform data of event A in Figure 1, recorded in low- and high-gain seismometers. The amplitude of coda decreases exponentially with time, and the coda in low-gain records is subject to digitizing round-off error at long lapse time. Thus, high-gain records are used for the analysis of coda.

widely applied to array data since its introduction (e.g., Capon, 1973). The application here to source arrays is justified by the principle of source–receiver reciprocity (Aki and Richards, 1980). The source-array  $f$ - $k$  approach was found to be useful for studies to investigate the nature of wave fields in the source region (e.g., Spudich and Bostwick, 1987; Hong and Xie, 2005).

Each regional phase has unique phase velocity. Thus, wavelets with the same phase velocity may develop as the same seismic phase. For instance,  $S_n$  wavelets can be radiated simultaneously in different directions from a single source, and they develop as  $S_n$  phases in the different azimuths. The seismic coda is constituted by scattered wavelets that may be radiated in various directions from the source. As we examine the constituent energy of coda, we define the consistent energy arrival of the same phase as coherent energy.

The phase velocities and azimuths of waves leaving the source arrays can be estimated by staking discrete slowness power spectra over a finite frequency band (Hong and Xie, 2005):

$$P_w(\mathbf{s}) = \frac{1}{N} \sum_{j=1}^N |U(\omega_j \mathbf{s}, \omega_j)|^2 / m_j, \quad (1)$$

where  $\omega_j$  ( $j = 1, 2, \dots, N$ ) is a discrete frequency,  $N$  is the number of discrete angular frequencies,  $\mathbf{s}$  is a slowness vector, and  $U$  is a discrete double-Fourier spectrum of array waveforms. The parameter  $m_j$  is a normalization (whitening) factor that corrects for the instrument response and seismic attenuation (Hong and Xie, 2005).

Theoretically, every phase radiated from the sources can be tracked using a source-array analysis. Even wavelets that are scattered from stationary heterogeneities can be tracked as long as they are coherent over UNE records. Thus, using the source-array  $f$ - $k$  analysis of seismic coda, we can resolve the original phases of scattered wavelets, regardless of their post-phase types after scattering (Hong and Xie, 2005). Here, because the source-array analysis is based on a set of seismograms recorded at different times, energy from temporal sources is identified as inconsistent energy. This feature makes it easy to assess actual scattered energy. However, multiple scattering makes the scattered wave field diffused, and nonstationary background noises interfere with the scattered wave field. In this situation, the original phases of diffused scattered wavelets may not be well identified from the source-array analysis.

After the  $f$ - $k$  analysis, coherent energy of a specific phase is retrieved from array records using beamforming based on slant stacking (Kanasewich, 1981; Matsumoto *et al.*, 1998). The beamforming is operated for all azimuthal directions (i.e., from  $0^\circ$  to  $360^\circ$ ). This beamforming of the source-array records collects unimodal wavelets, leaving the sources in a given azimuthal direction. This analysis allows us to quantify the energy of a specific phase as a function of the radiation direction from the sources.

### Configuration of Source Array

The aperture of the source array is  $\sim 19$  km in the longitudinal direction (Fig. 1). The average depth of burial is 465 m below the surface. The standard deviation of depths,  $\Delta d$ , is 73 m. The average interval between adjacent UNEs,

$l_a$ , is 1.42 km. The variation of focal depths is sufficiently small compared to the event interval,  $\Delta d/l_a = 0.051$  so that the source-array components can be assumed to be placed on a horizontal plane. The error caused by inhomogeneous depth of burials can be neglected when the wavelength of analyzed phase  $\lambda_p$  is sufficiently larger than the variation in depth of burials of array components ( $\Delta d$ ) such that  $\lambda_p > 4\Delta d$  (Spudich and Bostwick, 1987). This relationship leads to

$$f_p < \frac{v}{4\Delta d}, \quad (2)$$

where  $f_p$  is the frequency of phase, and  $v$  is the phase velocity.

The phase  $Rg$ , the fundamental-mode Rayleigh wave at regional distance, has the lowest phase velocity among regional phases. From equation (2), the critical condition for unaliasing analysis of  $Rg$  is  $f < 8.5$  Hz. This critical condition sets the upper frequency limit of regional-phase analysis. However, the critical frequency is greater than the Nyquist frequency of data set (5.2 Hz). Considering the Nyquist frequency and the frequency contents of regional waves (Hong and Xie, 2005), we limit the analysis by 3.2 Hz in this study. Thus, the aliasing effect from spatial variation of array components is avoided in our analysis. The response functions of the source array are well concentrated in the centers for four different frequency ranges (Fig. 3), which indicates a high resolution of array analysis at the given frequency bands.

### Analysis of Phase Composition

A source-array  $f$ - $k$  analysis examines the dominant original phase and its dominance in the array records. When the strengths of phases are comparable among various phases, multiple peaks appear in the slowness power spectrum. If the constituent wavelets at a time window are direct phases from the source to receiver, the angles of the multiple peaks in the slowness power spectrum should correspond to the azimuth between the sources and receiver. Thus, we can examine the radiation directions and phase velocities of wavelets leaving the sources, which allows us to investigate the temporal variation of coda composition. In addition, we can infer the influence of scattering on the construction of seismic coda. When multiple scattering is dominant, the wave field becomes diffusive, and the coherency of phases over array records decreases. In such cases, slowness power spectra may display multiple peaks that are inconsistent with time.

A diffuse field is stochastically equivalent to a static wave field composed of infinite numbers of standing modal waves. Here the modal amplitudes can be arbitrary (Lobkis and Weaver, 2001). Physically, this corresponds to a system with multiple secondary sources that are distributed densely in the medium (Snieder, 2004). In the Earth, the multiple secondary sources correspond to heterogeneities that radiate scattered wavelets. Thus, the construction of diffuse field

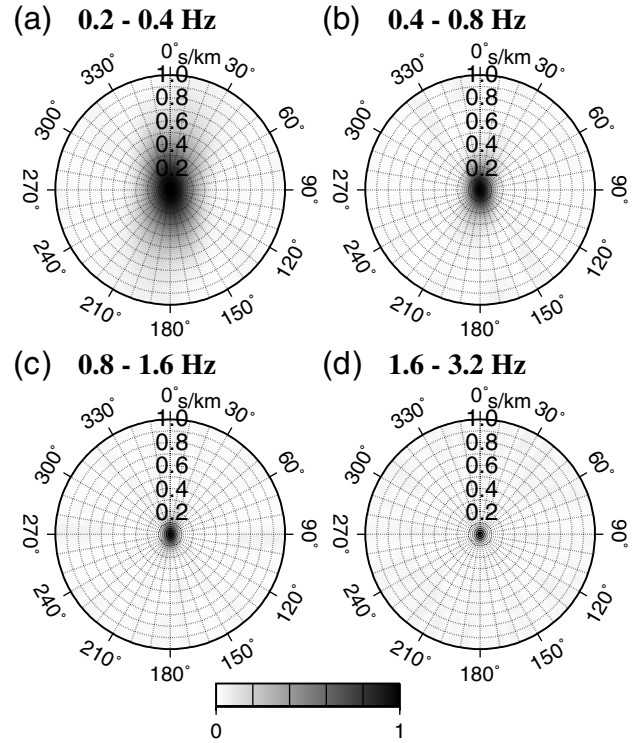


**Figure 3.** Array response functions of the source array for various frequency bands: (a) 0.2–0.4 Hz, (b) 0.4–0.8 Hz, (c) 0.8–1.6 Hz, and (d) 1.6–3.2 Hz. The energy is concentrated in the centers of slowness power spectrum diagrams, which indicates a high-resolving power of  $f$ - $k$  analysis without any noticeable aliasing effects.

depends on constitutional phases and their propagation directions.

In this study, the variation of phase contents is examined by frequency bands. Considering the typical frequency contents of regional phases and the resolution of source array (Hong and Xie, 2005), we set four frequency ranges, 0.2–0.4, 0.4–0.8, 0.8–1.6, and 1.6–3.2 Hz. The coda sections are band-pass filtered before source-array analysis.

We observe strong and coherent scattered energy with a phase velocity of 3.0 km/sec in the slowness power spectra at frequency bands of 0.2–0.4 and 0.4–0.8 Hz (Fig. 4b). This phase velocity corresponds to the typical  $Rg$  phase velocity in this region (Hong and Xie, 2005). Also, the frequency range (0.2–0.8 Hz) in which the  $Rg$  energy is observed is consistent with the reported  $Rg$  frequency content. This  $Rg$  phase is consistently observed over the entire coda section of array records with a duration of 900 sec, which corresponds to about four times the  $Rg$  travel time and an  $Rg$  propagation distance of about 2700 km.

The observed  $Rg$  energy is quantified by beamforming the source-array records. The distribution of  $Rg$  energy as function of radiation direction is given in Figure 5. The azimuthal angles of the maximum  $Rg$  energy are not constant, but keep varying with time. The indicated angles are appar-



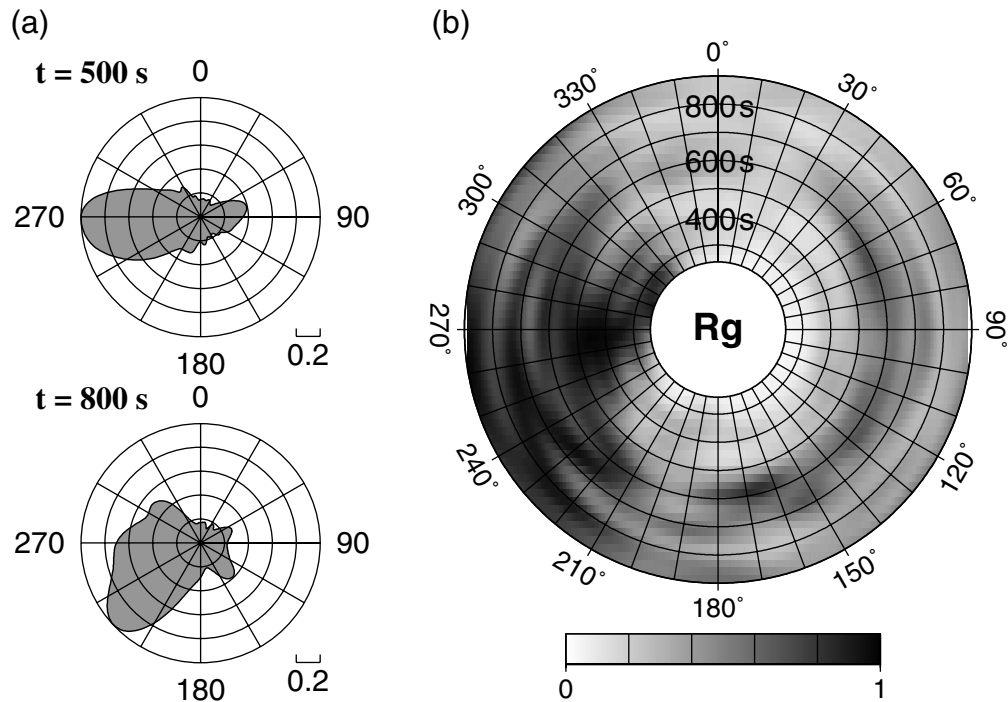


**Figure 5.** (a) Azimuthal distributions of normalized  $R_g$  scattered energy at lapse times of 500 and 800 sec. The  $R_g$  scattered energy is quantified using a slant stacking. (b) Collective results of normalized  $R_g$  scattered energy at lapse times from 245 to 900 sec. The azimuths of maximum strength, which indicate the initial radiation directions from the source, vary with time. The temporal variation of azimuths indicates that  $R_g$  waves are scattered from various sources of lateral heterogeneities distributed over regional and teleseismic distances.

ently different from the azimuth between the sources and receiver ( $\sim 303.9^\circ$ ). This difference in angles suggests that the energy was not radiated initially in the direction of the great-circle path, but was radiated in a deviated direction. This observation implies multipathing propagation.

We examine every coda record section, and confirm no apparent interference of other sources. Also, because we adopt source-array records that are collected in different times, any temporal sources are well suppressed in the source-array analysis. Thus, this expectation suggests that the observed energy is partitioned from  $R_g$  energy because of scattering (Fig. 6). These  $R_g$ -origin scattered waves are observed only after the direct  $R_g$  phase, but not before the direct  $R_g$ . On the other hand, the coda after major regional phases such as  $P_n$  and  $L_g$  phases displays the phase velocities of the preceding phases (Hong and Xie, 2005). These observations suggest that phase-coupled scattered energy from  $R_g$  is not so strong as to interfere with the scattered energy from other phases.

We, however, do not find any dominant phases in high-frequency coda (0.8–1.6 Hz and 1.6–3.2 Hz). The phases and radiation directions are observed to be distributed randomly over the slowness-azimuth domain (Fig. 4d). This complex phase composition lasts over the entire coda. The multiple random peaks support that the high-frequency coda is not composed of any consistent phases. Thus, it appears that

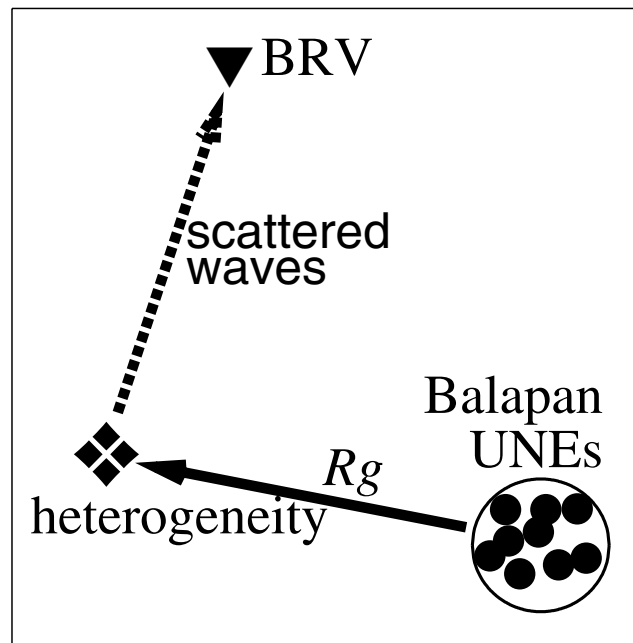


**Figure 6.** Schematic diagram for observation of  $R_g$  energy radiated in outside the great-circle direction because of scattering.

the high-frequency coda is well mixed with various scattered waves of comparable strengths, which causes the wave field to be diffusive (Del Pezzo *et al.*, 1997). Here, the comparable strengths of phases in high-frequency regime suggest that major body-wave phases are attenuated significantly with scattering, unlike the  $Rg$  phase that is still dominant in the low-frequency range.

### Constituent Energy

We quantify the scattered energy in terms of regional phases to estimate the influence of individual phase on the construction of regional coda. The scattered energy is quantified by assessing the slowness power spectra. We con-

sider three regional phases,  $P$ ,  $S$ , and  $Rg$  (Fig. 7). We set the  $P$  slowness range to include  $Pn$  and  $Pg$  energy, and the  $S$  slowness range is set to include  $Sn$  and  $Lg$  energy. The applied  $P$  slowness range is 0.12–0.17 sec/km, the  $S$  slowness range is 0.20–0.25 sec/km, and the  $Rg$  slowness range is 0.29–0.42 sec/km.

We first estimate the background diffusive energy level in the coda. The surplus amount of coherent energy in the coda can be estimated by correcting for the background diffusive energy. The unidentifiable scattered waves that are in diffused states constitute 80% of the total coda energy in 0.2–0.4 Hz, in which regional  $Rg$  phase is most dominant. The  $Rg$ -origin energy composes 10%–18% (~14% on average) of coda energy in the frequency range, while  $P$ - and  $S$ -origin

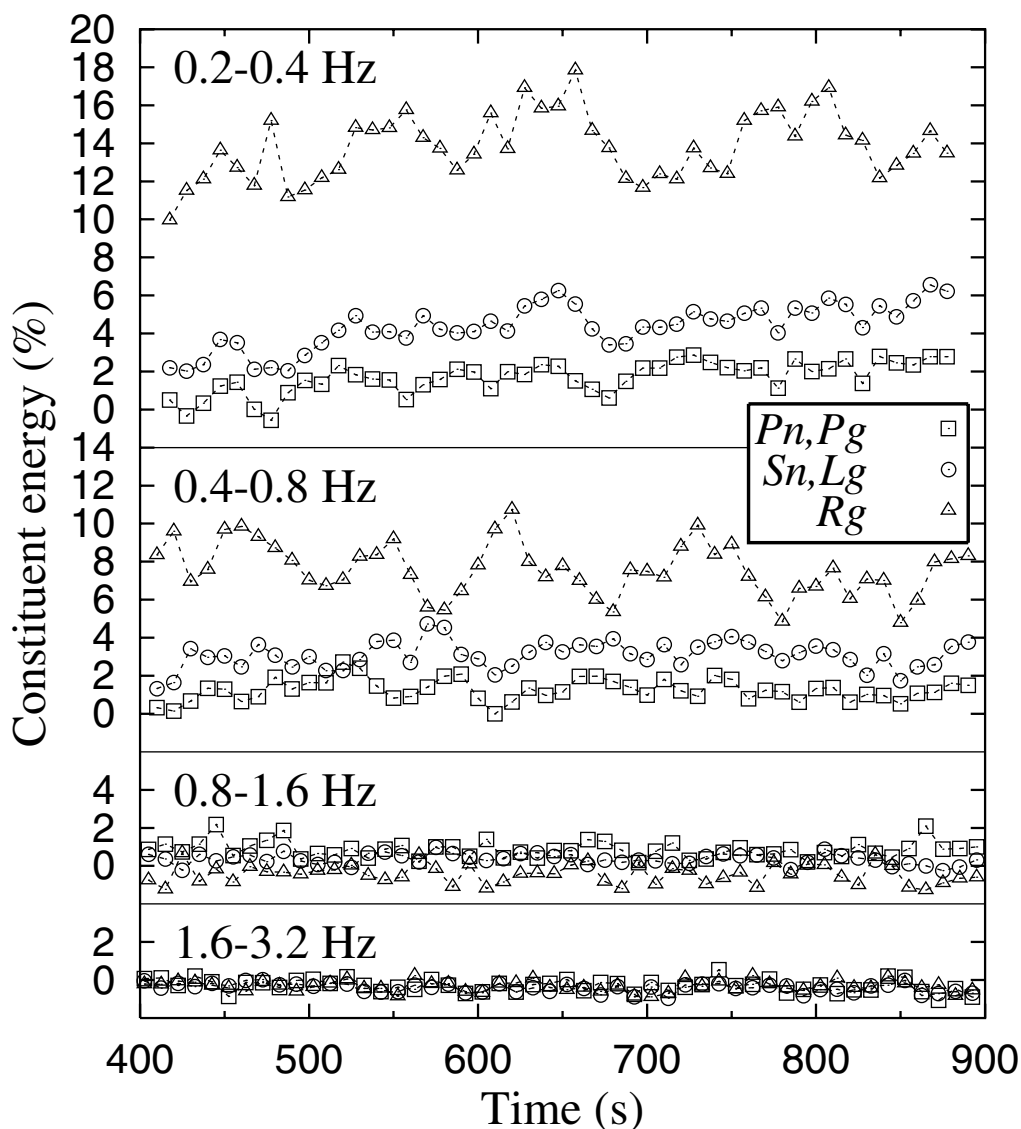


**Figure 7.** Constituent energy of seismic coda in terms of regional phases.  $Rg$ -origin energy dominantly constitutes low-frequency coda (0.2–0.4 Hz; 0.4–0.8 Hz). In higher frequencies (0.8–1.6 Hz; 1.6–3.2 Hz), the phases of origin are barely identified, which may be associated with multiple scattering by small-scale heterogeneities in the crust. The high-frequency coda appears to be diffusive.

energy constitutes only 0%–2% (~1% on average) and 2%–5% (~3% on average), respectively. We thus find that the coherent energy in the coda decreases with frequency. For coda of 0.4–0.8 Hz, the *Rg* phase constitutes 6%–11% (~8% on average). The energy from the other phases constitutes 0%–4%. On the other hand, the constituent phases are observed to be complex in the higher frequencies of 0.8–1.6 Hz and 1.6–3.2 Hz.

The observation in high-frequency range suggests that the constituent wavelets were originated from multimodal phases. This phase composition leads to construct a diffuse field (Lobkis and Weaver, 2001). The observation of energy from major regional phases at low-frequency coda, but rare at high-frequency coda, may be related to the frequency-dependent nature of scattering; the magnitude of scattering is strong when the wavelength is comparable to the size of heterogeneity (Sato and Fehler, 1998; Hong, 2004; Hong *et al.*, 2005). High-frequency waves interact strongly with the small-scale heterogeneities in the crust and mantle lid. Low-frequency waves, on the other hand, respond less to the small-scale heterogeneities. Note that the dimension of small-scale changes with depth because the wavelength,  $\lambda$ , increases with the wave velocity,  $c$  (i.e.,  $\lambda = c/f$ , where  $f$  is the frequency).

It is intriguing that the *Rg*-origin energy lasts to the end of the low-frequency coda. This observation suggests that *Rg*-origin energy constitutes a significant portion of the low-frequency coda, which agrees with the phase composition of scattered wave field near the free surface (Hennino *et al.*, 2001). The dominance of *Rg*-origin energy over other phases in the low-frequency coda may be caused by the difference in geometrical spreading; the travel distances of *Rg* are much shorter than those of body waves arriving simultaneously. This feature agrees with the recent observation of Rayleigh-wave retrieval from cross correlation between regional seismic coda of a pair of stations (Campillo and Paul, 2003; Shapiro *et al.*, 2005). The group velocities of the Rayleigh waves can be directly inverted for the Green's function of the medium. The retrieval of Green's function from cross correlation of seismic noises was confirmed by both theoretical and numerical studies (Roux *et al.*, 2005; Weaver and Lobkis, 2005; Paul *et al.*, 2005).

The observed energy constitution of regional coda, thus, explains the reason why only Rayleigh waves are retrieved instead of body-wave phases such as *Pn* and *Sn*. The Rayleigh energy is observed only up to a frequency of 0.8 Hz in this study. Thus, it appears that the Rayleigh-wave retrieval from coda cross correlation is possible at a low-frequency range. In other words, the retrieval of a specific phase is expected to be fairly limited in a high-frequency regime because of the nature of regional coda. From these observations, the equipartition approximation (mixture of multimodal waves) in coda analysis appears to be particularly suitable for analysis of high-frequency coda (Shapiro *et al.*, 2000).

## Discussion and Conclusions

We have examined the phase composition of regional coda and studied the contribution of regional phases on the construction of regional coda. The original phases of scattered wavelets could be identified using a source-array analysis technique. Underground nuclear explosions provide a unique set of uniform sources that are essential for source-array analysis.

Strong and coherent *Rg*-origin energy lasts continuously to the end of coda (more than 700-sec lasting coda) in a low-frequency range of 0.2–0.8 Hz. This *Rg*-origin energy is dominant over the energy from other regional phases. The *Rg*-origin energy is the most influential component that prevents the low-frequency coda from being diffused. Identifiable regional phases constitute about 20% of coda energy in a frequency range of 0.2–0.8 Hz. The other 80% of coda energy is composed of diffusive scattered waves. The *Rg*-origin energy is mostly observed only after the arrival time of the direct *Rg*. The observation suggests that *Rg*-to-*Rg* scattering is a dominant process in the low-frequency scattered wave field.

In higher frequency ranges ( $f > 0.8$  Hz), the constituent energy of coda is observed to mixed with multimodal phases. This intensive diffusion of coda at high frequencies may be related with the presence of crustal heterogeneities that interfere strongly with high-frequency waves. The equipartition approximation based on diffuse field that is often applied in coda analysis appears to be particularly suitable for high-frequency coda.

## Acknowledgments

We thank Jiakang Xie for valuable discussions on the  $f$ - $k$  analysis of source-array data. We are grateful to Won-Young Kim, Vitaly Khalturnin, and Paul Richards for information on Balapan explosion data. We thank Robert Nowack and an anonymous reviewer for their constructive comments. This work was supported by the Korea Meteorological Administration Research and Development Program under Grant Number CATER 2007-5111.

## References

- Aki, K., and B. Chouet (1975). Origin of coda waves: source, attenuation, and scattering effects, *J. Geophys. Res.* **80**, 3322–3342.
- Aki, K., and P. G. Richards (1980). *Quantitative Seismology, Theory and Methods*, Vol. 1, W. H. Freeman, New York.
- Bianco, F. M., M. Castellano, E. Del Pezzo, and J. M. Ibanez (1999). Attenuation of short-period seismic waves at Mt. Vesuvius, Italy, *Geophys. J. Int.* **138**, 67–76.
- Bonner, J. L., D. C. Pearson, W. S. Phillips, and S. R. Taylor (2001). Shallow velocity structure at the Shagan River test site in Kazakhstan, *Pure Appl. Geophys.* **158**, 2017–2039.
- Campillo, M., and A. Paul (2003). Long-range correlations in the diffuse seismic coda, *Science* **299**, 547–549.
- Capon, J. (1973). Signal processing and frequency–wavenumber spectrum analysis for a large aperture seismic array, in *Methods in Computational Physics*, B. A. Bolt (Editor), Vol. 13, Academic, New York, 1–59.
- Capon, J. (1974). Characterization of crust and upper mantle structure under LASA as a random medium, *Bull. Seismol. Soc. Am.* **64**, 235–266.

- Del Pezzo, E., M. La Rocca, and J. Ibanez (1997). Observations of high-frequency scattered waves using dense arrays at Teide volcano, *Bull. Seismol. Soc. Am.* **87**, 1637–1647.
- Frankel, A., and L. Wennerberg (1987). Energy-flux model of seismic coda: separation of scattering and intrinsic attenuation, *Bull. Seismol. Soc. Am.* **77**, no. 4, 1223–1251.
- Hedlin, M. A. H., P. M. Shearer, and P. S. Earle (1997). Seismic evidence for small-scale heterogeneity throughout the Earth's mantle, *Nature* **387**, 145–150.
- Hennino, R., N. Trégourès, N. M. Shapiro, L. Margerin, M. Campillo, B. A. van Tiggelen, and R. L. Weaver (2001). Observation of equipartition of seismic waves, *Phys. Rev. Lett.* **86**, 3447–3450.
- Hong, T.-K. (2004). Scattering attenuation ratios of *P* and *S* waves in elastic media, *Geophys. J. Int.* **158**, 211–224.
- Hong, T.-K., and J. Xie (2005). Phase composition of regional seismic waves from underground nuclear explosions, *J. Geophys. Res.* **110**, B12302, doi 10.1029/2005JB003753.
- Hong, T.-K., R.-S. Wu, and B. L. N. Kennett (2005). Stochastic features of scattering, *Phys. Earth Planet. Interiors* **148**, 131–148.
- Hoshiya, M. (1997). Seismic coda wave envelope in depth-dependent *S*-wave velocity structure, *Phys. Earth Planet. Interiors* **104**, 15–22.
- Kanasewich, E. R. (1981). *Time Sequence Analysis in Geophysics*, Third Ed., Univ Alberta Pr, Edmonton.
- Kim, W.-Y., P. G. Richards, V. Adushkin, and V. Ovtchinnikov (2001). Technical Report: Borovoye digital seismogram archive for underground nuclear tests during 1966–1996, Lamont–Doherty Earth Observatory of Columbia University.
- Korn, M. (1993). Determination of site-dependent scattering *Q* from *P*-wave coda analysis with an energy-flux model, *Geophys. J. Int.* **113**, 54–72.
- Levashova, N. M., K. E. Degtyarev, M. L. Bazhenov, A. Q. Collins, and R. van der Voo (2003). Permian palaeomagnetism of East Kazakhstan and the amalgamation of Eurasia, *Geophys. J. Int.* **152**, 677–687.
- Lobkis, O. I., and R. L. Weaver (2001). Observation of equipartition of seismic waves, *J. Acoust. Soc. Am.* **86**, 3447–3450.
- Matsumoto, S., K. Obara, and A. Hasegawa (1998). Imaging *P*-wave scatterer distribution in the focal area of the 1995 *M*7.2 Hyogo-ken Nanbu (Kobe) earthquake, *Geophys. Res. Lett.* **25**, 1439–1442.
- Mayeda, K., and W. R. Walter (1996). Moment, energy, stress drop, and source spectra of western United States earthquakes from regional coda envelopes, *J. Geophys. Res.* **101**, 11,195–11,208.
- National Nuclear Centre of the Republic of Kazakhstan (NNCRK) (1999). Technical Report, contributed by the National Nuclear Centre of the Republic of Kazakhstan, *Proceedings of the Workshop on IMS Location Calibration*, Oslo, January 1999.
- Nishimura, T., K. Yoshimoto, T. Ohtaki, K. Kanjo, and I. Purwana (2002). Spatial distribution of lateral heterogeneity in the upper mantle around the western Pacific region as inferred from analysis of transverse components of teleseismic *P*-coda, *Geophys. Res. Lett.* **29**, no. 23, 2137, doi 10.1029/2002GL015606.
- Nowack, R., and W.-P. Chen (1999). Source-receiver reciprocity and empirical Green's functions from chemical blasts, *Bull. Seismol. Soc. Am.* **89**, 538–543.
- Paul, A., M. Campillo, L. Margerin, E. Larose, and A. Derode (2005). Empirical synthesis of time-asymmetrical Green functions from the correlation of coda waves, *J. Geophys. Res.* **110**, B08302, doi 10.1029/2004JB003521.
- Quin, H. R., and C. H. Thurber (1992). Seismic velocity structure and event relocation in Kazakhstan from secondary *P* phases, *Bull. Seismol. Soc. Am.* **82**, 2494–2510.
- Ringdal, F., P. D. Marshall, and R. W. Alewine (1992). Seismic yield determination of Soviet underground nuclear explosions at the Shagan River test site, *Geophys. J. Int.* **109**, 65–77.
- Roux, P., K. G. Sabra, W. A. Kuperman, and A. Roux (2005). Ambient noise cross correlation in free space: theoretical approach, *J. Acoust. Soc. Am.* **117**, 79–84.
- Sato, H., and M. Fehler (1998). *Wave Propagation and Scattering in the Heterogeneous Earth*, Springer, New York.
- Shapiro, N. M., M. Campillo, L. Margerin, S. K. Singh, V. Kostoglodov, and J. Pacheco (2000). The energy partitioning and the diffusive character of the seismic coda, *Bull. Seismol. Soc. Am.* **90**, 655–665.
- Shapiro, N. M., M. Campillo, L. Stehly, and M. Ritzwoller (2005). High-resolution surface-wave tomography from ambient seismic noise, *Science* **307**, 1615–1618.
- Snieder, R. (2004). Extracting the Green's function from the correlation of coda waves: a derivation based on stationary phase, *Phys. Rev. E* **69**, 046610.
- Spudich, P., and T. Bostwick (1987). Studies of the seismic coda using an earthquake cluster as a deeply buried seismograph array, *J. Geophys. Res.* **92**, 10,526–10,546.
- Thurber, C., C. Trabant, F. Haslinger, and R. Hartog (2001). Nuclear explosion locations at the Balapan, Kazakhstan, nuclear test site: the effects of high-precision arrival times and three-dimensional structure, *Phys. Earth Planet. Interiors* **123**, 283–301.
- Weaver, R. L., and O. I. Lobkis (2005). Fluctuations in diffuse field-field correlations and the emergence of the Green's function in open systems, *J. Acoust. Soc. Am.* **117**, 3432–3439.
- Yoshimoto, K., H. Sato, and M. Ohtake (1997). Three-component seismogram envelope synthesis in randomly inhomogeneous semi-infinite media based on the single scattering approximation, *Phys. Earth Planet. Interiors* **104**, 37–61.

Department of Earth System Sciences  
Yonsei University  
Shinchon-dong, 134, Seodaemooon-gu  
Seoul 120-749, South Korea  
tkhong@yonsei.ac.kr  
(T.-K.H.)

Lamont-Doherty Earth Observatory of Columbia University  
61 Route 9W  
Palisades, New York 10964  
(W.M.)

Manuscript received 9 May 2007